Journal of Modern Physics, 2023, 14, 1721-1734
https://www.scirp.org/journal/jmp
ISSN Online: 2153-120X
ISSN Print: 2153-1196

Meissner Exclusion of Gravito-Magnetic Energy from a Momentum-Space Crystal

Edwin Eugene Klingman

Cybernetic Micro Systems, Inc., San Gregorio, CA, USA
Email: klingman@geneman.com

How to cite this paper: Klingman, E.E. (2023) Meissner Exclusion of Gravito-Magnetic Energy from a Momentum-Space Crystal. *Journal of Modern Physics*, **14**, 1721-1734.
https://doi.org/10.4236/jmp.2023.1413101

Received: November 8, 2023
Accepted: December 12, 2023
Published: December 15, 2023

Abstract

A primordial field theory of Quantum Gravity resolves a number of century-old paradoxes associated with general relativity and quantum mechanics. It allows re-interpretation of major experiments such as Michelson-Gale (1925) and Q-bounce (1999). I address herein an unexplained anomalous experiment by Martin Tajmar (2006), in terms of a gravitomagnetic-based Meissner effect.

Keywords

Quantum Gravity, Meissner Exclusion, Momentum Space Crystal, Gravitomagnetism, Tajmar Anomaly

1. Introduction

Any theory of Quantum Gravity faces an uphill climb, as evidenced in Arma's "*Conversations on Quantum Gravity*" [1]. A century of paradox accompanies 20th Century relativity and quantum theory, much of this due to the attempt to base the physics of space-time on geometry. Ashtekar says: "… *if in fact geometry is a physical entity*, *as Einstein has taught us… geometry should have an atomic structure*." Yet, Field states: "*Spacetime is just an abstraction… I believed all my life that spacetime exists*, *but I no longer do so*." Einstein early concluded [2] that space and time are abstractions; "*there is no vacuum* (aka 'empty space') *absent field*." Feynman, Weinberg and others, state that geometry is unnecessary as a means of understanding gravity, so much quantum gravity is based on geometrical concepts deemed inappropriate by some of our greatest physicists.

Every theory is intended to describe or explain physical reality. Instead of pursuing highly abstract conceptions, effectively divorced from physical reality, we assume that a fundamental physical field, the primordial field, came into existence at the Creation, the only physical reality in existence. The plan of this paper is:

1) Introduction
2) The Primordial Field of the Universe
3) Local C-field induced structure and energy distribution
4) Definition of Momentum-space Crystal
5) Meissner-exclusion of Gravitomagnetic field from Momentum-space Crystal
6) Primordial field explanation of Tajmar effect
7) Summary
8) Conclusions.

2. The Primordial Field of the Universe

If nothing else exists, evolution of the primordial field ψ can occur only through self-interaction, and this principle is reflected in the self-interaction equation:

$$\nabla\psi = \psi\psi : \left\{\psi(\xi) = -\xi^{-1}, \psi(\boldsymbol{\xi}) = \boldsymbol{\xi}^{-1}\right\} \tag{1}$$

where solutions are simply presented, and ∇ represents the change operator $\nabla = \partial_\xi$. Defining primordial field $\psi = \boldsymbol{G}(\boldsymbol{r},t) + i\boldsymbol{C}(\boldsymbol{r},t)$ with corresponding operator $\nabla = \boldsymbol{\nabla} + \partial_t$, Equation (1) becomes [3].

$$(\boldsymbol{\nabla} + \partial_t)(\boldsymbol{G} + i\boldsymbol{C}) = (\boldsymbol{G} + i\boldsymbol{C})(\boldsymbol{G} + i\boldsymbol{C}) \tag{2}$$

A Hestenes' Geometric Calculus expansion of this equation immediately leads to the following:

$$\begin{array}{ll} \textbf{Self-Interaction equations} & \textbf{Heaviside equations} \\ \boldsymbol{\nabla}\cdot\boldsymbol{G} = \boldsymbol{G}\cdot\boldsymbol{G} - \boldsymbol{C}\cdot\boldsymbol{C} & \boldsymbol{\nabla}\cdot\boldsymbol{G} = -\rho \\ i\boldsymbol{\nabla}\cdot\boldsymbol{C} = i2\boldsymbol{G}\cdot\boldsymbol{C} & \boldsymbol{\nabla}\cdot\boldsymbol{C} = 0 \\ \partial_t\boldsymbol{G} - \boldsymbol{\nabla}\times\boldsymbol{C} = \boldsymbol{G}\times\boldsymbol{C} \pm \boldsymbol{C}\times\boldsymbol{G} & \boldsymbol{\nabla}\times\boldsymbol{C} = -\rho\boldsymbol{v} + \partial_t\boldsymbol{G} \\ i\boldsymbol{\nabla}\times\boldsymbol{G} + i\partial_t\boldsymbol{C} = 0 & \boldsymbol{\nabla}\times\boldsymbol{G} = -\partial_t\boldsymbol{C} \end{array} \tag{3}$$

Heaviside's generalization of Newtonian gravity is equivalent (under iteration) to Einstein's GR. Terms on the left are given *field energy density* interpretation leading to Heaviside's (1893) formulation [4] of the right side of (3). The concept of *field strength* is absent in the derivation, other than the implicit assumption of ultra-strong fields existing at the big bang. The fields are shown in **Figure 1**. *Encoding Energy-Density as Geometry* [5] analyzes the mismatch between primordial field ontology and "geometric reality" and discusses the physical reality associated with such. After the conceptual basis of the theory has been developed, the theory has been used to re-interpret key experiments of physics such as the well-known (1925) Michelson-Gale [6] and (1999) Q-bounce experiments [7]. This paper advances the theory by applying it to an anomalous (2006) experiment by Martin Tajmar [8].

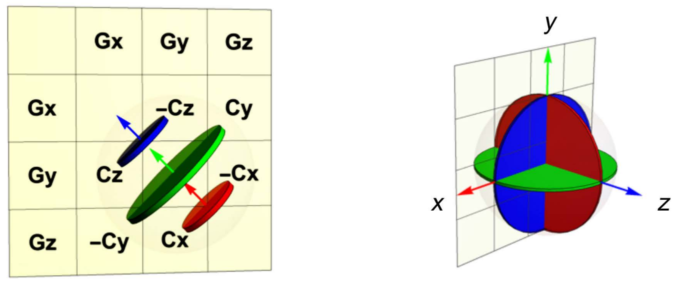

SU[2] = SU(3)

Figure 1. The circulating field, the C-field, can be labeled by the (row, col) component or by the orthogonal axis about which the (row, col) component circulates. For example, the (*x*, *z*) element is labeled C_y and the (*z*, *x*) element is labeled $-C_y$ since both of these terms rotate about the y-axis; similarly for the other components. These rotations are shown abstractly in the representation of the field strength $F_{\mu\nu}$ matrix on the left. The right-hand illustration maps the three bivector diagrams into 3-space. Colors are used for visual convenience and for suggested correlation with SU(3) × SU(2) × U(1) symmetry.

3. Local C-Field-Induced Structure and Energy Distribution

$$\boldsymbol{C}(x,y,z)=\sum\nolimits_{i=1}^{N}\boldsymbol{p}_i\times\boldsymbol{r}_i\Big/\int \mathrm{d}r_i^3 \tag{4}$$

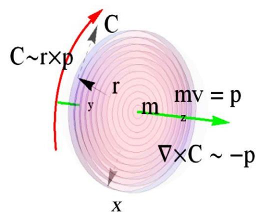

Consider a slice of local C-field induced by a momentum density $\boldsymbol{p}=\rho\boldsymbol{v}$. The diagram in Equation (4) depicts mass m, momentum $\boldsymbol{p}$ (green), circulating-C-field-slice (pinkish), and C-field circulation direction (red, curved arrow). C-fields are additive, however circulation is strongest near the momentum, so consider the fields of two relatively independent entities. As is evident from the red C-field curved arrow, for adjacent co-parallel momenta the chirality of the fields is such that they tend to cancel on the axis between them when added, as shown in **Figure 2(b)**, in which two momenta point out of the page, with their induced C-field calculated at surrounding points. On the line between two identical momenta, the field at the midpoint of the axis will be zero.

We make full use of the most powerful tools available to physicists [9] including Hestenes' *Geometric Calculus* (GC) [10] and Wolfram's *Mathematica 13+*, and potentially *ChatGPT-4* [11]; Although GC can be extended to arbitrary dimensions, ontological analysis implies that we are concerned only with three spatial dimensions $\{\hat{x},\hat{y},\hat{z}\}$ plus scalar time. Points are labelled $\{x,y,z,t\}$; GC-objects function in coordinate-free space and support scalars, 1D-points, 2D-bivectors, 3D-trivectors, and a pseudoscalar or duality operator, *i*, as in $\boldsymbol{a}\wedge\boldsymbol{b}=-i(\boldsymbol{a}\times\boldsymbol{b})$, which projects a plane into an orthogonal (dual) vector. Unlike most math, which does not mix apples and oranges, <u>all</u> GC-objects interoperate and interact algebraically. Arfken [12] shows that sometimes the local integral of an infinitesimal volume is equal to

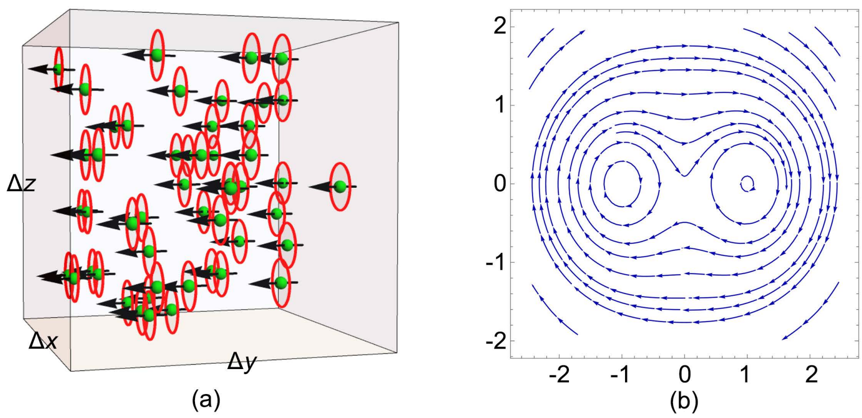

Figure 2. (a) Random atomic nuclei with common momentum density vectors distributed in local cube. (b) The C-field is summed around two nuclei with parallel momentum, perpendicular to the page. C-field cancellation occurs at the midpoint, but circulation around both particles form left-handed loops. The asymmetry is an artifact of the sampling instruction used to create the plot.

$$\int \mathrm{d}^3 x = \Delta x \Delta y \Delta z = \text{trivector} \tag{5}$$

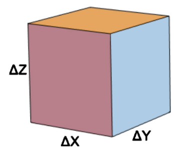

Thus, integration over a volume is sometimes equivalent to multiplying by the scaled volume. In Equation (5) we show the infinitesimal volume as integral formulation, as differential volume, as trivector, and geometrical equivalent. Specific boundary value problems defined on a volume containing distributed sources often require exquisite analytical integrations making use of Gauss' theorem, Stokes' theorem, and Cauchy's theorem. On the other hand, a region containing many particles and associated (entangled) fields, with density n per unit volume, need only be multiplied by the relevant volume. Therefore, when appropriate, we will explicitly depict the trivector in integral form, as in Equation (4).

Consider mass flowing through an infinitesimal volume: the momentum of any mass is essentially the momentum of the nuclei comprising the mass as seen in Figure 2(a) where particles are randomly distributed with all nuclei moving in $\boldsymbol{p}$ direction, but the nuclei are not locked in a lattice configuration; *thermal* motion is allowed in the plane perpendicular to $\boldsymbol{p}$. Integrating meaningful information sometimes equates to simply counting particles in a given region of space, each of which induces a local momentum-based field; interacting particles interact through their fields. Fields of left-handed co-parallel momenta conflict with each other, and vanish at the midpoint between the two, as shown in Figure 2(b).

Let us examine the way in which we plan to display the relevant C-field energy. Figure 3 depicts a number of momenta, located at [$x = \{1, 2, 3, 4\}$, $y = 0$, $z = 0$] and a line through the 2-D plane perpendicular to $\boldsymbol{p}$, left to right. We calculate the C-field vector at every point on the line by summing the contribution at

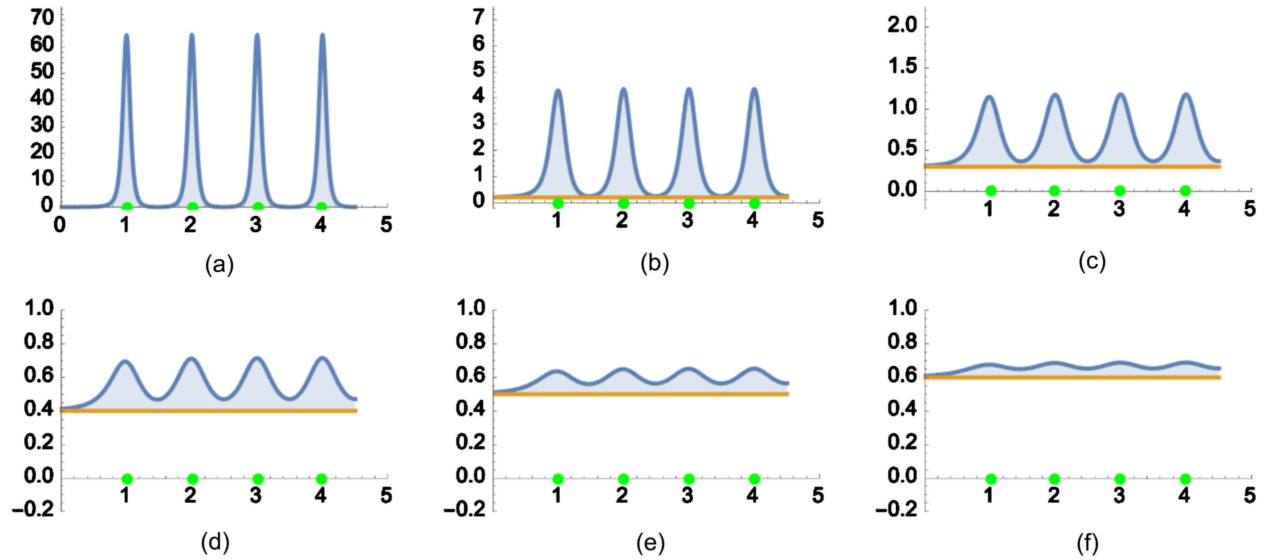

Figure 3. (a)-(f) C-field energy density for four (green) momenta on x-axis.

this point from each of the nuclei in the plane. The energy of the field is $\boldsymbol{C}(x,y,z)\cdot\boldsymbol{C}(x,y,z)$ sampled on the intersection of the $y=k$ plane and the $z=0$ plane.

C-field energy surrounding mass in motion is shown around individual nuclei; local field energy is largely contained inside the cube. Figure 2(b) shows two parallel momenta perpendicular to the plane of the page, each inducing a left-handed C-field circulation, such that fields vanish exactly halfway between the particles, while above and below the particles the field circulates more or less in the same direction, indicated by arrows on the contour lines. Having computed $\boldsymbol{C}(x)$ for every point on a line, we compute local energy density at the points on the line by calculating $|\boldsymbol{C}(x)\cdot\boldsymbol{C}(x)|$. In Figure 3, the base line is orange, drawn at height k above the momenta, and amplitude of the C-field energy density at the point on the orange line is given by the blue curve. The sampling curve vanishes midway between two momenta, as shown for two momenta in Figure 2(b), due to y-components of neighboring momenta cancelling each other. As we rise above the momenta, up and down C-field components tend to cancel, whereas horizontal C-field components add in the *+x* direction (above the momenta), and in the *-x* direction if we are sampling below the momenta.

It is easy to visualize the density contours for two source fluxes (momentum density $\rho\boldsymbol{v}$). It is more difficult to study the density contours for all of the momenta in the cube in Figure 2(a). Figure 4 shows three rows of diagrams, each a random displacement from lattice points. Each row shows density profiles across four slices.

4. Definition of Momentum-Space Crystal

Ontologically, a cube of mass is not solid mass, but consists of atoms with electrons

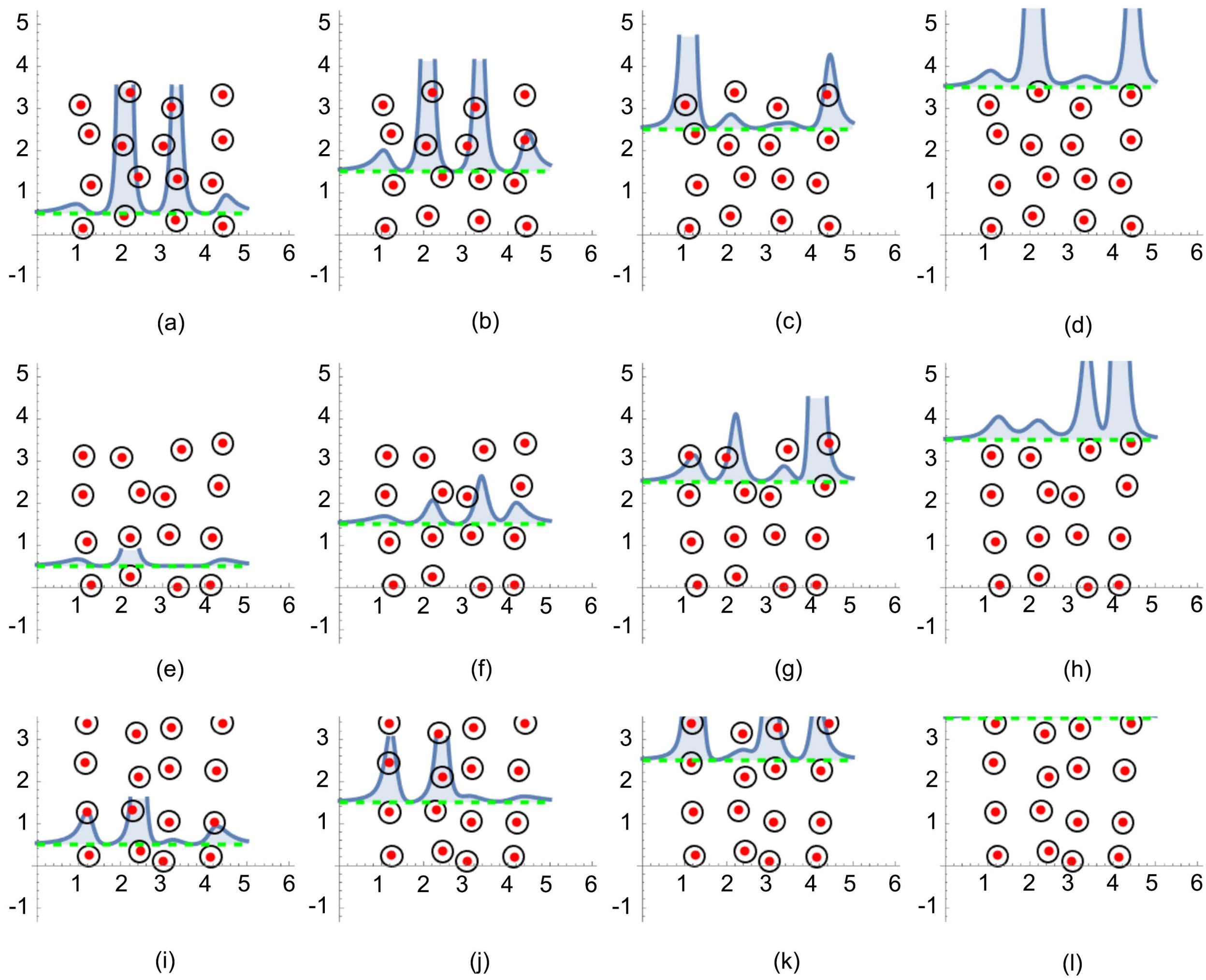

Figure 4. (a)-(l): A 4 × 4-array with random displacements from the 4 × 4 lattice points. The C-field energy density is sampled on lines midway between rows of lattice points. Randomly arranged momenta yield random C-field energy density distributions across the array, that is, the C-field energy varies within the material.

and nuclei. Clouds of electrons keep nuclei distributed evenly over local space but contribute very little to momentum density $\rho \boldsymbol{v}$ where $\rho = m \big/ \int \mathrm{d}^3 x$ and $m = \sum m_{nucleus}$. Ideally, the nuclei are positioned at equidistant lattice points, however the ideal is frustrated by thermal motion. Thus, if we cool the material, we expect the average positions of nuclei to move closer to the lattice points. In the limit, identical momenta located at the lattice points define a momentum-space crystal. Depending upon constitution of the lattice, different lattices "freeze" at different temperatures, for example, Wang *et al.* [13] describe a particular lattice freezing below 50 K. To investigate the C-field behavior of momenta at the lattice points, we consider two rows of momenta, located at $y = 0$ and $y = 1$ as shown in **Figure 5(a)**, sampled as described by Equation (6), with $k = \frac{1}{2}$.

$$\boldsymbol{C}(x, y, z) = \sum_{i=1}^{ncol} \sum_{j=1}^{nrow} r3\left[x - x_{ij}, y = k, 0\right] \times \left\{0, 0, p_z\right\} \tag{6}$$

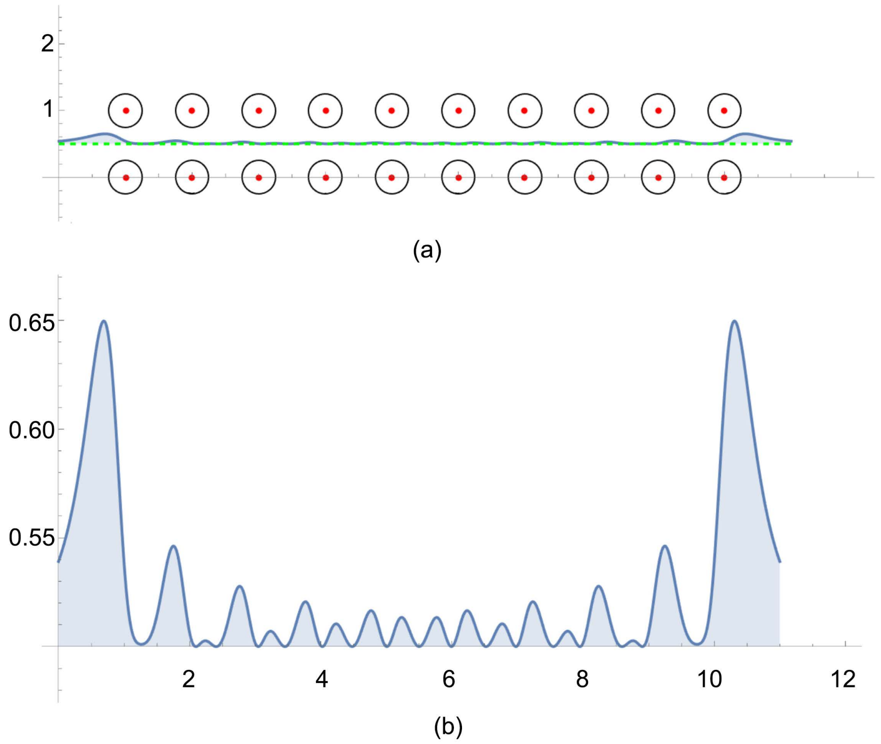

Figure 5. (a) C-field sampled online midway between rows of momenta shows cancellation of circulation. In (b) the sampled energy density diagram is expanded (from $y = 0.5$ to $y = 0.64$) demonstrating that much of the C-field energy density has been excluded from the material.

5. Discussion of Tajmar Effect

Martin Tajmar and de Matos began exploring gravitomagnetism in conjunction with the London moment of superconductivity. The BCS Theory of superconducting related "Cooper pairs" of electrons whose anomalous mass was not understood; electron's charge and mass occurs in relevant equations, but it's unclear whether electron mass or *bare* mass accounts for apparent mass increase of niobium Cooper pairs, though they differ by about three orders of magnitude.

Tajmar and others spun rings of various materials in a cryogenically cooled container and used accelerometers and later laser gyroscopes to detect the gravitomagnetic field generated when the angular velocity of the spinning ring is varied. These detectors are positioned inside the ring and at three positions above the rings with detectors in mirror pairs (the "curl configuration") to cancel mechanical signals. The spin vector of the disk points down and establishes the clockwise or counterclockwise direction of the field. The experiment varied the materials, the temperatures, and the velocity profiles, as seen in **Figure 6**. As expected, the gravitomagnetic field varies directly proportional to the applied angular acceleration of the ring, and the direction of the peak signal changes with the sense of rotation. Niobium gave the strongest acceleration in the tangential direction when angularly accelerated, with gravitational peaks observed when the superconductor passed its critical temperature while rotating.

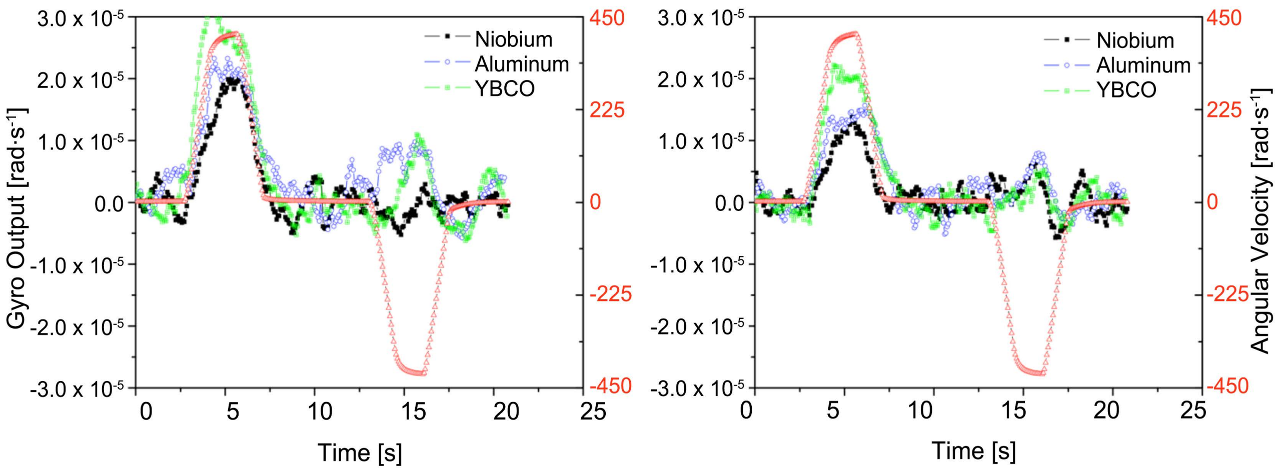

Figure 6. Laser Gyro output for Niobium, Aluminum, and YBCO versus *Applied Angular Velocity* (Δ) between a Temperature of 4 - 6 Kelvin. (a) LG 1 (Reference); (b) LG 2 (Middle).

An unexpected result was the detection of parity: the gyro outputs show a parity violation between clockwise and counterclockwise rotation (the CW signal is larger than the CCW signal), independent of the gyro's orientation. At 4 K and a top speed of 420 rad/s the anomalous gyro signal is as large as one third of the Earth's signal. The gyro follows the applied angular velocity, but only if the ring is rotated in the clockwise orientation. For example, at 4.2 K they performed 40 successive clockwise rotations, and the gyro effect could always be measured. Then (again at 4.2 K) they performed 40 CCW rotations, but any effects were an order of magnitude reduced compared to CW results. In any case, an independent experiment using the world's most precise laser gyro (in a different experiment configuration) shows the gyro's response to the speed of the spinning superconductor, but the parity violation is greater for the counterclockwise rotation—the *opposite* of the above experiments. The fact that the Canterbury ring laser experiment was carried out in the southern hemisphere, while the above experiments were carried out in the northern hemisphere, suggests the origin of the parity effect is Earth's C-field-inducing rotation.

Figure 6(a) depicts the reference Laser Gyro while Figure 6(b) shows the signal from another Laser Gyro that is placed further above the spinning disk, and is therefore yields a weaker signal.

In 2006 Tajmar, Plesescu, Marhold, and de Matos, [14] reported that the niobium ring:

"*reached 30 orders of magnitude higher than what general relativity predicts classically*!"

In 2008, Tajmar, Plesescu, and Siefert [15] concluded that the gyro signal follows the rotating ring velocity with high correlation.

"*Compared to classical frame-dragging spin-coupling predictions, our signals are up to 18 orders of magnitude larger.*"

Tajmar and others have written papers discussing their theory behind the experiment and the data from the experiments. Early in the game, Tajmar and de Matos attempted to formulate theoretical explanations, mostly focused on Cooper pairs of electrons, but also including *massive photons*. McCulloch's model was based on Unruh radiation. These efforts did not pan out, so effort shifted to excluding artifacts from the data; effort devoted to systems error analysis and quantification. In the end they claim that the likelihood is that these are real physical effects *without any classical explanation so far*. In (2011) *Gravity Probe B* proved the existence of the C-field [16].

Primordial Field Theory is subject to the self-interaction principle, represented by self-interaction Equation (1) and nowhere supports a formulation of "field strength". In fact, as implied by the big bang assumption, the equation governs ultra-strong fields. Nevertheless, Einstein Geometers conceive of dropping higher order terms to linearize his GR equations, $R_{ij}-\frac{1}{2}Rg_{ij}=T_{ij}$, as producing the [erroneous] "weak field approximation". In [17] Tajmar and de Matos begin:

"*Using the weak field approximation, we can express the theory of general relativity in a Maxwell-type structure comparable to electromagnetism.*"

They follow this with: "*The volume integrals in* Equations (*9*) *and* (*12*) *assume point masses.*"

I believe assumption of the "weak field approximation" and assumption of "point masses" preclude a proper ontological understanding of the Primordial Field Theory and its conceptualization of the Meissner effect of "flux exclusion". In the *Momentum-space Crystal* analysis note that each line between rows of momenta shows suppressed C-field energy density in the interior of the crystal; the C-field flux energy excluded from the interior appears outside of the crystal.

6. Meissner Exclusion of Gravitomagnetic Field from Crystal

The Meissner Effect (1933) is typically associated with the total exclusion of any electromagnetic flux from the interior of a superconductor. It is one of the defining features of superconductivity. In the above we have postulated the exclusion of gravitomagnetic flux from the interior of a "frozen lattice of momenta". We have not made any assumptions about superconductivity associated with the C-field but will find an interesting correlation of C-field exclusion and superconductivity when we analyze the Tajmar anomaly. Knorzer, *et al.* [18] remark:

"*Electron-phonon interactions lie at the heart of several phenomena in condensed matter physics, including Cooper pairing* (…) *Generally, the low-energy excitations of electrons in solids are modified by this coupling to lattice vibrations, which alters the transport and thermodynamics behavior.*"

McColloch [19] notes that the Tajmar anomaly is an unexplained acceleration observed by gyroscopes close to, but isolated from, rotating rings cooled to 5 K. The Tajmar effect…

"…*is similar to the Lense-Thirring effect* (*frame-dragging*) *predicted by General Relativity but is* ***20 orders of magnitude larger*** *and shows the added parity violation.*"

This was initially called the gravitomagnetic London effect, but it has been

"…*discredited because the inception of the Tajmar effect* (*at about 25 K*) *does not coincide with the superconducting transition temperature*, *only with very low temperatures.*"

Thus, in agreement with our common sense or intuition the C field is not absolutely banished from the 2D array but vanishes midway between the neighboring momenta as seen in Figure 7. We multiply the energy of two rows by N to sum the energies excluded between $N+1$ rows of frozen momenta (Figure 8). Here we show only 10 momenta per row. The same approach works for N_{col} momenta per row but smooths out the energy "bumps" between the rows.

The diameter of the niobium atom is approximately 150 picometers or 0.15 nanometers. Since the material is approximately 15 mm thick, then we determine the number of rows as follows:

$$\frac{15\times10^{-3}}{150\times10^{-12}}=\frac{1}{10}\times10^{9}=10^{8}\quad\text{rows of niobium atoms}$$

This is where the 10^8 arises.

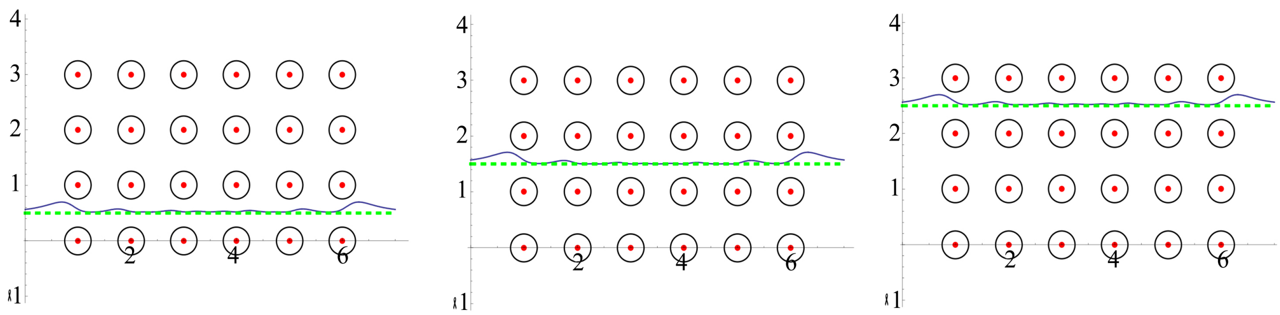

Figure 7. Clarifying the situation for a 4 × 6 momentum array. The left diagram shows the field as sampled *midway* between the first and second rows of momentum. As expected, the field is excluded. Next, we sample the field **midway** between the second and third row of momentum. Again, the field vanishes due to the inherent cancellation of the chiral circulation.

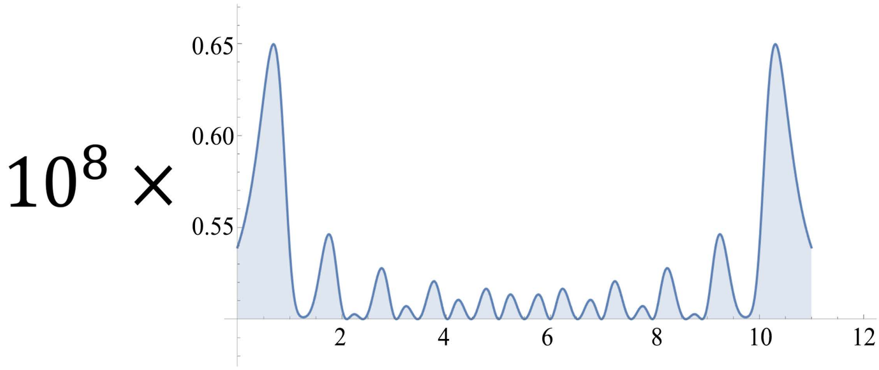

Figure 8. Depicting the multiplication of energy per row times the number of rows.

7. Summary

The primordial Equation (1) has two parametric solutions, a scalar and a vector. In Hestenes' *Geometric Calculus* these are dual with complex "i" the duality operator. When treated as such, Heaviside's equations are derived from the primordial field equation. Heaviside derived his gravitational equations from Newton's equation in analogy with Maxwell's electromagnetic equations, which are satisfied for $E + iB$ where E is the electric field and B is the magnetic field. Heaviside's $G + iC$ represents gravity field G and gravito-magnetic field C, both of which are physical fields that have been experimentally detected; the C field by NASA's 2011 *Gravity Probe B* experiment.

Primordial field $\psi = \boldsymbol{G} + i\boldsymbol{C}$ energy density is proportional to field amplitude squared, $\sim \boldsymbol{G} \cdot \boldsymbol{G}$ and $\sim \boldsymbol{C} \cdot \boldsymbol{C}$. Gravitational field $\boldsymbol{G}$ is effectively constant over the measurement device, whereas gravito-magnetic field $\boldsymbol{C}$ at any point in local space is the sum of the local fields induced by local momentum, in this case the momentum density of the atomic nuclei [*niobium*]. When the nuclei are perfectly arranged on the (crystal) lattice, the field midway between the rows of nuclei cancel, and local field energy is minimum. In **Figure 4**, the nuclei are not in a perfect lattice arrangement [due to thermal motion] and therefore do not cancel at every midway point between the rows. The positioning of the nuclei is essentially random, so the local field at the midway point is effectively random, and the square of the local field is energy density, shown as the shaded portion between the green midway line and the blue energy density line. As shown in **Figure 5** and **Figure 7**, when nuclei are positioned at the lattice points, internal energy is minimized, and the gravito-magnetic field is *excluded* from the material. When this occurs for superconducting materials, the exclusion of the magnetic field is known as the Meissner effect. Tajmar's experiments proved that gravito-magnetic field energy density ($\sim \boldsymbol{C} \cdot \boldsymbol{C}$) is excluded so I interpret this as *a gravitomagnetic Meissner effect*. No other interpretation has successfully explained Tajmar's results.

A reviewer stated that the "change operator" seems weird and asks if it has any physical meaning. It is designed to emulate standard physics equations, relating changes in one field to interactions with parameterized sources. Since the primordial field is the *only* field existing at the big bang, then it can interact only with itself, and this leads to the primordial field self-interaction equation, which has two formal solutions, as shown in Equation (1). We intuitively associate the scalar parameter as *time* and the vector parameter as *position* in space, and this leads to the Heaviside interpretation of gravity. What about emergent phenomena? If the primordial field is the *only* field in existence at the big bang, and today's universe has evolved/emerged from the big bang, then the entire universe we live in today has *emerged* from this field equation. A number of my papers describe key examples of emergent phenomena; the gravito-magnetic Meissner effect observed in this paper is such a key example.

The reviewer claims that cosmological and astrophysical aspects emerge from quantum gravity (that may be true, although it has not yet been shown to be true) and wonders about the effects described in this manuscript and quantum gravity. The Meissner effect is a quantum gravity effect in primordial field theory, derived from Equation (1). This topic is explored in reference [7], "*The Ontology of Quantum Gravity*", wherein the quantum wave function is interpreted to be the induced gravito-magnetic wave, *a real physical field*, whereas the quantum "wave function" of today's quantum gravity is unknown—no one is sure whether the nature of the wave function is epistemological (abstract) or ontological (physically real). As for the question, "any unification?", the primordial field unifies the physics of the universe, with examples of such unification presented in paper after paper, with more to come. As for "What is gravity?", as noted initially, there is no need for a geometric interpretation of gravity; the *G*-field solution to the primordial equation is Newton's gravitational field, and the gravito-magnetic *C*-field is Heaviside's gravito-magnetic analogy with electro-magnetism. These emerge as the primordial field at the big bang.

In summary, primordial field theory is not an abstract theory based on mathematics; it is an ontological theory of physical reality, based on the appearance of a universal primordial physical field, quickly shown to be compatible with Newton's gravity and Maxwell's electromagnetism. Unlike today's key theories—which are essentially paradoxical and incomplete, with no unified representation—primordial field theory does not give rise to paradoxes (logical inconsistencies) and is believed to unify quantum theory, gravitational physics, and particle physics. Some of this has been demonstrated in previous papers, some is yet to be presented.

8. Conclusions

Ontological concepts of "weak field approximation" to general relativity and "point masses" preclude proper ontological understanding of gravitomagnetism. Point masses have very little mass but "infinite" mass density. "Weak fields" place unrealistic limits on linearized gravity. Primordial field theory does not mention "field strength"—it applies to <u>all</u> field strengths equally. For example, the strength of the C-field circulation is determined by the momentum density, *i.e.*, the velocity of the relevant mass density. This concept fails when "point mass" is assumed. For extended particles (such as neutrons) finite densities yield C-field wave functions appropriate to quantum gravity, and field strengths at particle levels that have been ignored for over a century, due to the erroneous conception of "weak field approximation". The circulation induced by linear velocity is identical to kinetic energy, *i.e.*, energy previously linked to "motion" exists as C-field circulation. Normally, C-field circulation <u>inside</u> a solid mass is not measurable, per se, but our analysis of the primordial field leads to "flux exclusion" of the sort measured by Tajmar, de Matos, and others. The result is seen to be many orders of magnitude greater than that predicted by general relativity, with its "weak field" assumption.

Early experimenters assumed that Meissner-like flux exclusion occurred at onset of superconductivity. McColloch points out however that "*the inception of the Tajmar effect* (*at about 25 K*) *does not coincide with the superconductivity transition temperature*." I interpret this as follows:

The "freezing of the lattice" applies to the niobium nuclei, with atomic number 41 and atomic weight 92.906. Pure niobium is a superconductor when it is cooled below 9.25 K. The frozen lattice implies that the nuclei exist at lattice points and, as a result, exclude the C-field "flux" inside the material (except that immediately circling each nucleus' momentum). This behavior is uncoupled from superconductivity in the sense that the niobium nuclei are ~169,000 more massive than electrons; therefore, it takes much less thermal energy to move electrons in random fashion. To get rid of this energy, it is necessary to continue to cool the material until the 9.25 K temperature is reached and niobium becomes superconducting, which is characterized by Meissner exclusion of electromagnetic fields from inside the material.

In conclusion, the experimenters claim that the likelihood is that these are real physical effects *without any classical explanation so far*, while the primordial field theory explains the Tajmar anomaly in quite sensible fashion, compatible with ontological aspects of C-field developed in a number of my earlier papers.

Conflicts of Interest

The author declares no conflicts of interest regarding the publication of this paper.

References

[1] Armas, J. (2021) Conversations on Quantum Gravity. Cambridge U Press, Cambridge. https://doi.org/10.1017/9781316717639

[2] Einstein, A. (1952) Relativity: The Special and General Theory. Crown Publishers Inc., New York.

[3] Klingman, E. (2021) *Journal of Modern Physics*, **12**, 65-81. https://www.scirp.org/journal/jmp https://doi.org/10.4236/jmp.2021.122007

[4] Heaviside, O. (1893) *The Electrician*, **31**, 281-282.

[5] Klingman, E. (2021) *Journal of Modern Physics*, **12**, 1190-1209. https://doi.org/10.4236/jmp.2021.129073

[6] Klingman, E. (2023) *Journal of Modern Physics*, **14**, 1003-1017. https://doi.org/10.4236/jmp.2023.146055

[7] Klingman, E. (2023) *Journal of Modern Physics*, **14**, 1392-1408. https://doi.org/10.4236/jmp.2023.1411080

[8] Tajmar, M. and de Matos, C. (2003) *Physica C*, **385**, 551-554. https://doi.org/10.1016/S0921-4534(02)02305-5

[9] Klingman, E. (2023) *Journal of Applied Mathematics and Physics*, **11**, 514-524. https://doi.org/10.4236/jamp.2023.112031

[10] Hestenes, D. and Sobczyk, G. (1984) Clifford Algebra to Geometric Calculus. Reidel Pub., Boston. https://doi.org/10.1007/978-94-009-6292-7

[11] Klingman, E. (2023) *Open Journal of Philosophy*, **13**, 531-543. https://doi.org/10.4236/ojpp.2023.133035

[12] Arfkin, G. (1966) Mathematical Methods for Physicists. Academic Press, New York.

[13] Wang, J., *et al*. (2022) *Physical Review Letters*, **128**, Article ID: 157202. https://doi.org/10.1103/PhysRevLett.128.134101

[14] Tajmar, M., *et al*. (2006) Experimental Detection of the Gravitomagnetic London Moment.

[15] Tajmar, M., Plesescu, F. and Seifert, B. (2008) *Journal of Physics*: *Conference Series*, **150**, Article ID: 032101. https://doi.org/10.1088/1742-6596/150/3/032101

[16] Everitt, C., *et al*. (2011) *Physical Review Letters*, **106**, Article ID: 221101. https://doi.org/10.1103/PhysRevLett.106.221101

[17] Tajmar, M. and de Matos (2001) Coupling of Electromagnetism and Gravitomagnetism in the Weak Field Approximation.

[18] Knorzer, J., *et al*. (2022) *Physical Review Letters*, **128**, Article ID: 120404. https://doi.org/10.1103/PhysRevLett.128.120404

[19] McColloch, M. (2018) The Tajmar Effect from Quantized Inertia.